



**UNIVERSIDAD REGIONAL AMAZÓNICA IKIAM**

Facultad de Ciencias de la Vida

Ingeniería en Biotecnología

Photocatalytic reduction of nitrate by a bismuth-based  
nanostructured photocatalyst

Angélica María Navarrete Vega

Tutor: Jan Spengler, PhD

Tena, marzo 2022

Napo, Ecuador

## Declaración de derecho de autor, autenticidad y responsabilidad

Tena, 29 de septiembre de 2021

Yo, Angélica María Navarrete Vega con documento de identidad N°1752769925, declaro que los resultados obtenidos en la investigación que presento en este documento final, previo a la obtención del título de Ingeniería en Biotecnología son absolutamente inéditos, originales, auténticos y personales.

En virtud de lo cual, el contenido, criterios, opiniones, resultados, análisis, interpretaciones, conclusiones, recomendaciones y todos los demás aspectos vertidos en la presente investigación son de mi autoría y de mi absoluta responsabilidad.

Por la favorable atención a la presente, suscribo de usted,

Atentamente,

Firma:



---

Angélica María Navarrete Vega

## **Certificado de dirección de trabajo de integración curricular**

Certifico que el trabajo de integración curricular titulado: “Photocatalytic reduction of nitrate by a bismuth-based nanostructured photocatalyst”, en la modalidad de: proyecto de investigación en formato artículo original), fue realizado por: Angélica María Navarrete Vega, bajo mi dirección.

El mismo ha sido revisado en su totalidad y analizado por la herramienta de verificación de similitud de contenido; por lo tanto, cumple con los requisitos teóricos, científicos, técnicos, metodológicos y legales establecidos por la Universidad Regional Amazónica Ikiám, para su entrega y defensa.

Tena, 29 de septiembre de 2021

Firma:



.....

Jan Spengler

C.I: 1757762099

## **AGRADECIMIENTOS**

Agradezco a mi familia, en especial a mis padres Román Navarrete y Norma Vega, quienes gracias a su apoyo y amor incondicional me han permitido culminar con este paso tan importante en mi vida.

Mención especial requiere el Doctor Jan Spengler, tutor y director del proyecto “Nanotecnología verde para la eliminación de amoníaco y nitrato en agua”, quien me acogió dentro de su grupo de investigación y a quien agradezco por la enseñanza brindada y recomendaciones para mi crecimiento profesional.

Agradezco al grupo #BiOX (subproyecto de Hi Water) en especial a Damián Tuba y Michael Suarez quienes me ayudaron y confortaron en cada uno de los procesos de la realización de este trabajo.

De la misma forma agradezco al Ing. Miguel Quishpe Quisphe y Andrea Salgado, técnicos de laboratorio de Geociencias quienes me brindaron constantes asesoramientos en cada uno de los pasos a seguir en cada etapa del proyecto. Un agradecimiento especial a Marcela Cabrera, técnica de Laboratorio Nacional de Referencia de Agua, por el apoyo y seguimiento en el desarrollo de este trabajo de investigación.

Este trabajo se realizó gracias al financiamiento del proyecto INEDITA (Programa Nacional de Financiamiento para Investigación): Nanotecnología verde para la eliminación de amoníaco y nitrato en agua. PIC-18-INE-IKIAM-001

**Angélica Navarrete**

## ÍNDICE GENERAL

Declaración de derecho de autor, autenticidad y responsabilidad .....	i
Certificado de dirección de trabajo de integración curricular.....	ii
AGRADECIMIENTOS .....	iii
ÍNDICE GENERAL.....	iv
ÍNDICE DE FIGURAS.....	v
ÍNDICE DE TABLAS .....	v
RESUMEN.....	vi
ABSTRACT .....	vii
Graphical abstract .....	1
Abstract .....	1
<b>1. Introduction.....</b>	<b>2</b>
<b>2. Materials and Methods .....</b>	<b>3</b>
2.1. Catalyst preparation.....	3
2.2. Catalyst characterization.....	4
2.3. Photoactivity experiments .....	4
2.4. Photocatalytic reduction of nitrate .....	4
2.5. Selectivity of Photoreduction of NO <sub>3</sub> <sup>-</sup> .....	5
<b>3. Results and Discussion.....</b>	<b>6</b>
3.1. Structure and chemical characterization .....	6
3.2. Optical properties .....	8
3.3. Photoactivity of BiOI microspheres.....	9
3.4. Photocatalytic reduction of nitrate .....	10
3.4.1. Effect of the photocatalyst dosage .....	10
3.4.2. Effect of addition of hole scavenger .....	11
3.5. Selectivity of the photocatalytic reduction of NO <sub>3</sub> <sup>-</sup> .....	13
<b>4. Conclusions.....</b>	<b>16</b>
<b>References .....</b>	<b>17</b>
<b>Supplementary Information.....</b>	<b>20</b>

## ÍNDICE DE FIGURAS

<b>Fig 1.</b> XRD patterns of BiOI sample.....	6
<b>Fig 2.</b> SEM image (a), diameter distribution (b), TEM image (c), and EDS analysis (d) of BiOI microspheres.....	8
<b>Fig 3.</b> Plot of $(F(R_{\infty}) \cdot h\nu)^{1/\gamma}$ versus the photon energy ( $h\nu$ ).....	9
<b>Fig 4.</b> Effect of BiOI dosage on photocatalytic reduction of 10 ppm of nitrate under visible light irradiation (a), and changes of pH during de reaction (b). ....	11
<b>Fig 5.</b> Effect of formic acid concentration as a hole scavenger on photocatalytic reduction of 10 ppm of nitrate using 0.13 g of BiOI under visible light illumination. ....	13
<b>Fig 6.</b> Concentration curve of $\text{NO}_3^-$ , formed $\text{NO}_2^-$ and $\text{NH}_4^+$ plotted as a function of irradiation time with 0.008 M of formic acid and 0.13 g of BiOI. ....	16

## ÍNDICE DE TABLAS

<b>Table 1.</b> Removal efficiency and selectivity of photocatalytic reduction using BiOI microspheres.....	14
---	----

## RESUMEN

La eliminación de nitratos es de gran importancia en los sistemas de tratamiento de aguas debido a sus impactos negativos, desde la eutrofización hasta el riesgo inmediato para la salud humana. La fotocatalisis ha surgido como un prometedor proceso de tratamiento de agua para superar este problema, ya que puede utilizar la luz solar para degradar los contaminantes. En este contexto, se han sintetizado microesferas fotocatalíticas de oxioduro de bismuto. Los productos se han caracterizado mediante DRX, SEM, TEM, EDS y espectroscopia de reflectancia difusa UV-VIS. Se investigó el efecto de las dosis de fotocatalizador (0,03, 0,06 y 0,13 g) en la reducción fotocatalítica del nitrato. La mayor reducción fotocatalítica se obtuvo en presencia de 0,13 g de BiOI, alcanzando un porcentaje de reducción del 57% tras 3 horas de irradiación bajo luz visible. También se demostró el importante papel del ácido fórmico como captador de agujeros para el proceso de reducción de nitratos. Se probaron diferentes concentraciones de ácido fórmico (0,002, 0,004 y 0,008 M) y se observó una mayor reducción cuando la concentración fue de 0,008 M. Estos resultados muestran que las microesferas de BiOI pueden utilizarse como prometedores fotocatalizadores impulsados por luz visible para la degradación de contaminantes inorgánicos, como el nitrato.

**Palabras clave:** nitrato, fotocatalisis, microesferas, fotorreducción, luz visible

## **ABSTRACT**

Nitrate removal is of great importance in water treatment systems due to its negative impacts, from eutrophication to the immediate risk to human health. Photocatalysis has emerged as a promising water treatment process to overcome this problem, because it can use the sunlight to degrade the pollutants. In this context, bismuth oxyiodide photocatalytic microspheres have been synthesized. The products were characterized by XRD, SEM, TEM, EDS and UV-VIS diffuse reflectance spectroscopy. The effect of photocatalyst dosages (i.e., 0.03, 0.06, 0.13 g) on the photocatalytic reduction of nitrate was investigated. The highest photocatalytic reduction was obtained in presence of 0.13 g of BiOI, achieving a reduction percentage of 57% after 3 hours of visible light irradiation. The important role of formic acid as a hole scavenger for the nitrate reduction process was also demonstrated. Different concentrations of formic acid were tested (0.002, 0.004, 0.008 M) and it was observed a highest reduction when the concentration was 0.008 M. These results show that BiOI microspheres can be used as promising visible-light-driven photocatalysts for the degradation of inorganic pollutants, such as nitrate.

**Key words:** nitrate, photocatalysis, microspheres, photoreduction, visible light

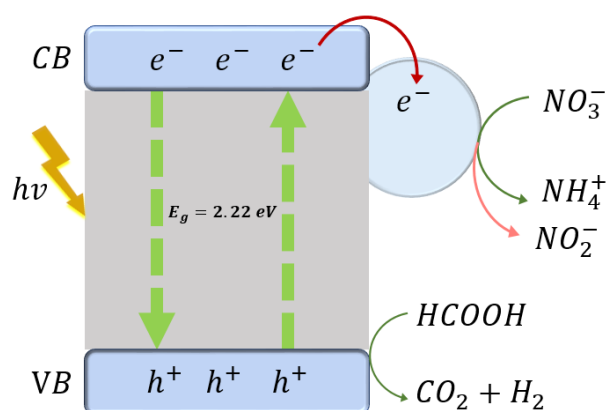
## Photocatalytic reduction of nitrate by a bismuth-based nanostructured photocatalyst

Navarrete A.<sup>1</sup>, Tuba D.<sup>2</sup>, Suarez M.<sup>1</sup>, Spengler J.<sup>1</sup>.

<sup>1</sup>Facultad de Ciencias de la Vida, Universidad Regional Amazónica Ikiam, Km 7, vía Muyuna, Tena, Napo, Ecuador.

<sup>2</sup>Facultad de Ciencias de la Tierra, Universidad Regional Amazónica Ikiam, Km 7, vía Muyuna, Tena, Napo, Ecuador.

### Graphical abstract



### Abstract

Nitrate removal is of great importance in water treatment systems due to its negative impacts, from eutrophication to the immediate risk to human health. Photocatalysis has emerged as a promising water treatment process to overcome this problem, because it can use the sunlight to degrade the pollutants. In this context, bismuth oxyiodide photocatalytic microspheres have been synthesized. The products were characterized by XRD, SEM, TEM, EDS and UV-VIS diffuse reflectance spectroscopy. The effect of photocatalyst dosages (i.e., 0.03, 0.06, 0.13 g) on the photocatalytic reduction of nitrate was investigated. The highest photocatalytic reduction was obtained in presence of 0.13 g of BiOI, achieving a reduction percentage of 57% after 3 hours of visible light irradiation. The important role of formic acid as a hole scavenger for the nitrate reduction process was also demonstrated. Different concentrations of formic acid were tested (0.002, 0.004, 0.008 M) and it was observed a highest reduction when the concentration was 0.008 M. These results show that BiOI microspheres can be used as promising visible-light-driven photocatalysts for the degradation of inorganic pollutants, such as nitrate.

**Key words:** nitrate, photocatalysis, microspheres, photoreduction, visible light

## 1. Introduction

Nitrate has become one of the most common contaminants in water supplies, especially groundwater[1]. Naturally, nitrate ion is produced in geological formations. However, its concentration has increased due to the indiscriminate use of nitrogen fertilizers in agriculture, contaminating water to such an extent that it is unsafe for human consumption[2]. Nitrate can have harmful effects on human health, including diseases, such as cancer derived from carcinogenic nitrosamines, and infant methemoglobinemia [3]. In addition, nitrate has effects on the environment because it can be a contributor to eutrophication and algal blooms[1].

Several treatment processes have been proposed for the management of nitrates in water, including physical (e.g., reverse osmosis, ion-exchange, adsorption), chemical (e.g., chemical denitrification, zero-valent metal nanoparticles, H<sub>2</sub> driven catalytic denitrification), electrochemical (e.g., electrocoagulation, electrodialysis, electrochemical reduction), and biological processes [4]. Although these processes have proven to be efficient for the reduction of nitrate (NO<sub>3</sub><sup>-</sup>), they still exhibit some drawbacks, such as incomplete removal of NO<sub>3</sub><sup>-</sup> and its hazardous reaction by-products (e.g., NO<sub>2</sub><sup>-</sup>, NH<sub>3</sub>) [4]. In order to ensure the safe of water, nitrate must be converted up to molecular nitrogen (N<sub>2</sub>). Hence, the photocatalysis has been considered a suitable and potential process to overcome the aforementioned issue, and to improve the N<sub>2</sub> selectivity. Since, it can efficiently use solar energy to purify water at ambient conditions[5]. In this sense, some photocatalytic materials have been employed for nitrate reduction [6–12].

TiO<sub>2</sub> is the most widely used photocatalyst due to its low cost and non-toxicity. However, it is a UV-light-driven photocatalyst, which limits its practical application [13]. Therefore, new visible-light-driven photocatalysts, such as bismuth-based materials have been developed. [5]. BiOX (X = Cl, Br, I) semiconductors are examples of bismuth-based photocatalysts, which have exhibited outstanding photocatalytic activity [14–17]. Among BiOX photocatalysts, BiOI has resulted attractive for water treatment due to its high chemical stability, low charge recombination, and narrow band gap (about 1.6-2.0 eV) [18]. Interesting results have been obtained for the removal of pollutants with different BiOI structures. Di et al. [19] synthesized BiOI microspheres by the solvothermal method and used them to evaluate their photocatalytic activity for the decomposition of model

pollutants such as methyl orange (MO) and obtained a degradation percentage higher than 92% in a time of 180 min. Similarly, Wang et al. [20], synthesized BiOI microspheres and used them to evaluate the decomposition of methylene blue (MB) and phenol obtaining as a result a percentage of degradation of MB of 98% in 50 min and 94% of phenol in 6 hours.

In a recent study, bismuth oxyhalide nanosheets were used to reduce nitrate [21], however BiOI flower-like microspheres have not been studied for this purpose. It has been found that BiOI microspheres with a flower-like morphology can have a higher photocatalytic efficiency compared to other bismuth oxyhalide nanostructures (e.g., nanosheets) due to their porosity, large surface area, and strong visible light absorption [22].

Based on the aforementioned, the current work aims (1) to synthesize BiOI flower-like microspheres via a solvothermal method, (2) to characterize these synthesized structures using a suite of instrumental analysis techniques (X-Ray Diffraction, Scanning electron Microscopy, Transmission electron microscopy, UV-Vis Diffuse Reflectance Spectroscopy), and (3) to evaluate the photocatalytic activity of these structures in nitrate reduction.

## **2. Materials and Methods**

### **2.1. Catalyst preparation**

All reagents (Sigma-Aldrich, St. Louis, MO, USA) used were of analytical grade and used without further purification. In this work, BiOI microspheres were prepared by a solvothermal synthesis. An "A" solution was prepared by dissolving 1.45 g (3 mmol) of bismuth nitrate pentahydrate in 30 mL of ethylene glycol. Simultaneously, a "B" solution was prepared by dissolving 0.49 g (3 mmol) of KI in 30 mL of ethylene glycol. The solution "B" was added drop by drop (1 mL/min) into the solution "A" under magnetic stirring at 500 rpm for 30 minutes and then was transferred in a 100 mL Teflon autoclave. The autoclave was placed in an oven and heated for 18 h at 126 °C, and then cooled at room temperature. Finally, the precipitate was separated using vacuum filtration and washed 3 times with deionized water, 2 times with absolute ethanol, and 2 times with deionized water. The product obtained was a deep orange precipitate which was dried at 60°C for 24 hours.

## 2.2. Catalyst characterization

X-ray diffraction patterns of BiOI were obtained by using an X-ray diffractometer (Malvern Panalytical Empyrean) equipped with a copper X-ray tube ( $K\alpha$  radiation,  $\lambda = 1.54056 \text{ \AA}$ ). The XRD data was collected in the  $2\theta$  range from  $5^\circ$  to  $90^\circ$  with a scan rate of  $0.01^\circ$  at 45 kV, and 40 mA. The UV-vis diffuse reflectance spectra of the microspheres were obtained at room temperature using a Lambda 365 spectrophotometer (Perkin Elmer) equipped with an integrating sphere. The morphology and microstructure of the powder sample was investigated on a scanning electron microscope (SEM, Tescan Mira 3) and transmission electron microscope (TEM, FEI- Tecnai G20 Spirit Twin) equipped with an Eagle 4k HR camera, respectively. The elemental composition of the powder BiOI was analyzed by energy-dispersive X-ray spectroscopy (EDS) using a Bruker X-Flash 6-30 detector with a resolution of 123 eV at Mn  $K\alpha$ .

## 2.3. Photoactivity experiments

The capacity of the synthesized BiOI microspheres to be activated with white LED light was investigated in the degradation of Bisphenol A (BPA). The batch photoreactor (40 x 40 x 60 cm) used for the experiments (Fig. S1) was equipped with a 500 mL beaker (Diameter: 10 cm), a hotplate stirrer, and a 50 W white LED lamp (Fig. S2 shows the spectra of the lamp), located at 20 cm from the beaker. The experiments were performed using 0.5 g/L of the photocatalyst and 110 mL of BPA solution (10 ppm). Prior to irradiation, the solution was let in dark for 1 h under constant stirring to achieve the adsorption-desorption equilibrium between the pollutant and photocatalyst surface. Afterward, the solution was illuminated for 3 hours, and 11 mL of the sample was collected each 30 min. Finally, the concentration of BPA was measured in a UV-VIS-NIR spectrophotometer (Shimadzu, UV-3600 Plus) at 276 nm.

## 2.4. Photocatalytic reduction of nitrate

The  $\text{NO}_3^-$  photocatalytic reduction tests were performed in a batch photoreactor mentioned above. Before starting the reaction, the solution was sonicated for 1 hour to diminish the dissolved oxygen concentration and, thereby, to ensure a complete reduction of nitrate. For each experiment, the photocatalyst was suspended by magnetic stirring in an ultrapure water solution (260 mL) containing nitrate and formic acid. Potassium nitrate ( $\text{KNO}_3$ ) was used as the nitrate source in this investigation. The experimental design matrix includes a baseline experiment (pH = 2.5, initial nitrate concentration = 10 mg/L, initial

formic acid concentration = 0.004 M, photocatalyst dosage = 0.03 g). Furthermore, the effect of the photocatalyst dosage was analyzed using 0.03, 0.06, and 0.13 g of BiOI, keeping the concentration of formic acid at 0.004M. The second set of experiments were performed using 3 different concentrations of formic acid (i.e., 0.002, 0.004 and 0.008 M). In addition, photolysis test was performed to see the sensitivity of nitrate to light conditions. These experiments were performed during 4 hours (1 hour of darkness and 3 hours in visible light) and the pH of the solution was measured each 30 min. 10 mL samples were taken every 30 min and then centrifuged for 1 hour. Subsequently, 3 mL of the supernatant were filtered using a membrane (pore size of 0.22  $\mu\text{m}$ ) in order to remove completely the photocatalyst particles. Ion chromatograph (Shimadzu, Prominence) was used to measure nitrate and nitrite anions (Shodex anion column, SI-52 4E) and ammonium cations (Shodex cation column, YS-50), with conductivity detector (Shimadzu, CDD-10AVP). Mobile phase was 3.5 mM sodium carbonate ( $\text{Na}_2\text{CO}_3$ ) and the flow rate 0.8 mL/min.

## 2.5. Selectivity of Photoreduction of $\text{NO}_3^-$

The  $\text{N}_2$  selectivity for nitrate reduction is very important to prevent the accumulation of nitrite and ammonium in water bodies, which are harmful products to human health [23]. The  $\text{NO}_3^-$  removal efficiency ( $e$ ) and the catalytic selectivity ( $s$ ) of  $\text{NO}_3^-$ , into  $\text{NO}_2^-$ ,  $\text{NH}_4^+$  and  $\text{N}_2$  (denoted as  $s\text{NO}_2^-$ ,  $s\text{NH}_4^+$ , and  $s\text{N}_2$ ) are mathematically expressed in the following equations (eq. 1-4) [11]:

$$e = \frac{[\text{NO}_3^-]_0 - [\text{NO}_3^-]_t}{[\text{NO}_3^-]_0} \times 100 \quad (1)$$

$$\%s\text{NO}_2^- = \frac{[\text{NO}_2^-]_t}{[\text{NO}_3^-]_0 - [\text{NO}_3^-]_t} \times 100 \quad (2)$$

$$\%s\text{NH}_4^+ = \frac{[\text{NH}_4^+]_t}{[\text{NO}_3^-]_0 - [\text{NO}_3^-]_t} \times 100 \quad (3)$$

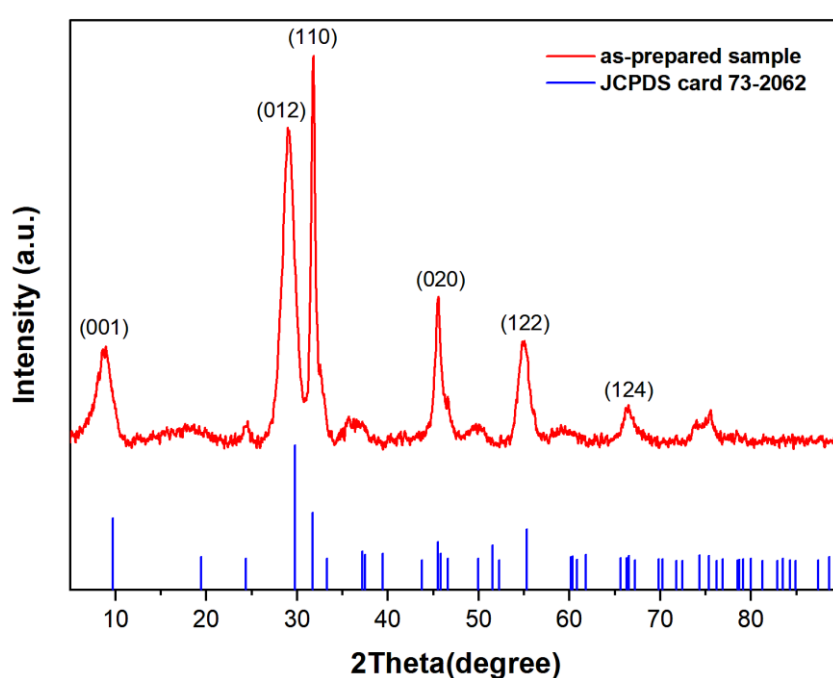
$$\%s\text{N}_2 = \frac{[\text{NO}_3^-]_0 - [\text{NO}_3^-]_t - [\text{NO}_2^-]_t - [\text{NH}_4^+]_t}{[\text{NO}_3^-]_0 - [\text{NO}_3^-]_t} \times 100 \quad (4)$$

Where  $[A]_0$  is the initial concentration of A ( $\text{NO}_3^-$ ,  $\text{NO}_2^-$  or  $\text{NH}_4^+$ ) and  $[A]_t$  is the concentration of A at time t. It was assumed that no by-products other than nitrite ( $\text{NO}_2^-$ ) and ammonium ( $\text{NH}_4^+$ ) are formed. This study is limited to the measurement of ions  $\text{NO}_3^-$ ,  $\text{NO}_2^-$  and  $\text{NH}_4^+$ .

### 3. Results and Discussion

#### 3.1. Structure and chemical characterization

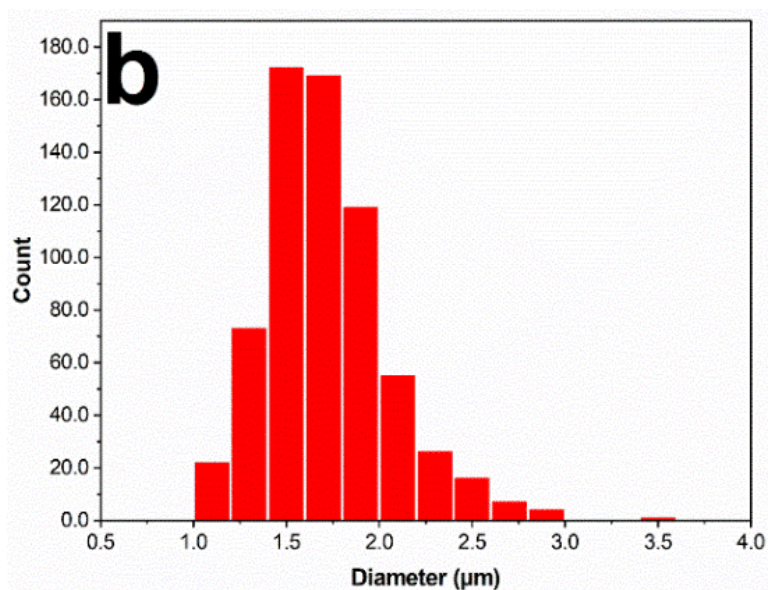
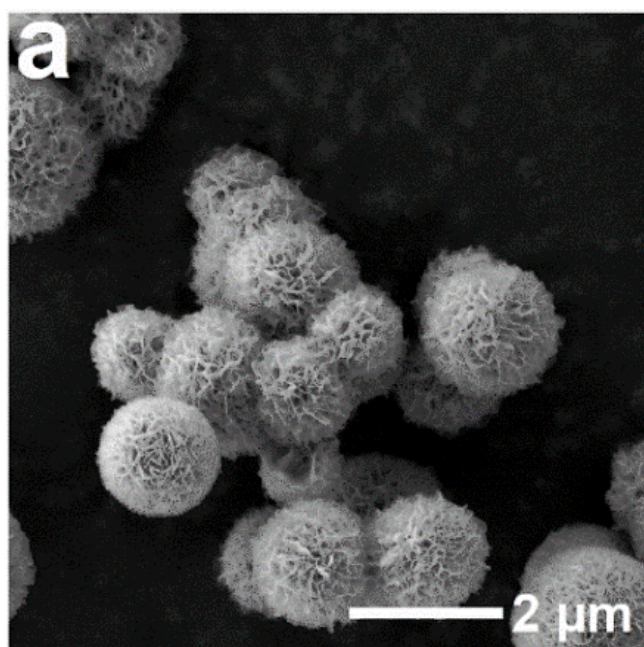
The crystal structure of the synthesized photocatalyst (BiOI) is shown in Fig. 1, the diffraction peaks are similar to those reported for the tetragonal phase of BiOI (JCPDS card 73-2062)[24]. No additional peaks to those reported were found, which indicates that the sample is pure. The synthesized BiOI sample shows an intense signal at  $2\theta = 31.7$ , which is assigned to the crystalline plane (110). It has been reported that BiOI structures with exposed {110} facets can exhibit a higher photocatalytic efficiency due to its ability to prevent the charge recombination and, thereby, to generate a higher amount of  $\cdot OH$  radicals [24].



**Fig 1.** XRD pattern of BiOI sample

As shown in Fig. 2a, the synthesized powder sample consists of microspheres with a flower-like morphology. From TEM image shown in Fig. 2c, it can be clearly observed that BiOI microspheres has a flower-like morphology. The diameter of the microspheres was determined by analyzing the SEM images with the software Image J. As shown in Fig. 2b, the microspheres have diameters ranging from 1.0  $\mu m$  to 3.45  $\mu m$ , and the average diameter was calculated to be  $1.717 \pm 0.329 \mu m$ . This morphology type exhibited by BiOI microspheres can provide a higher number of active sites available for photocatalytic reactions [24]. Moreover, the flower-like morphology can favor the separation of the

photogenerated electron/hole pairs, therefore, improving the photocatalytic activity [18]. Due to these facts, the photocatalytic reduction of nitrate molecules by BiOI flower-like microspheres could be conducted efficiently. On the other hand, the EDS analysis (Fig. 2d and Fig. S3) shows that the synthesized BiOI microspheres are composed of Bi, I, and O elements. Moreover, no signals corresponding to other chemical species were observed, suggesting that the compound is pure.



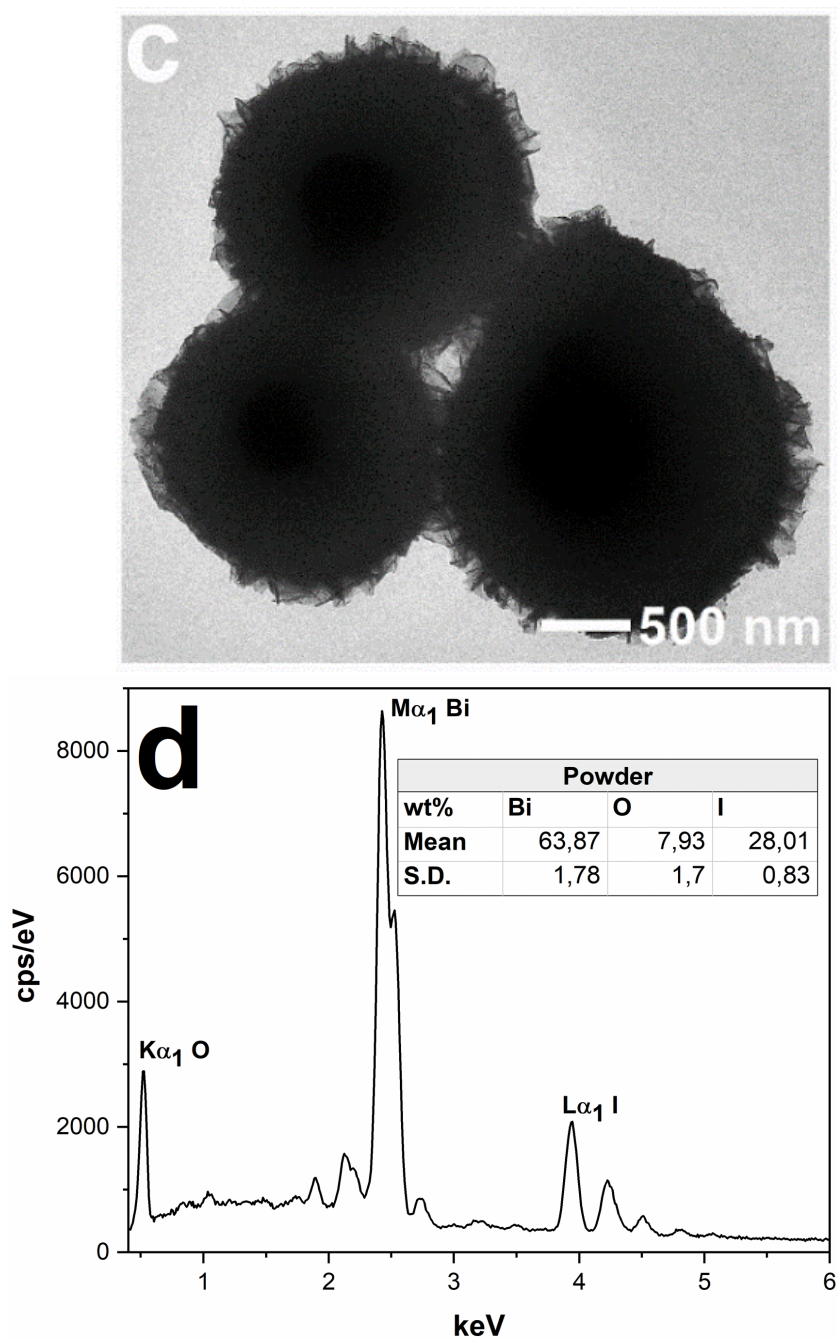


**Fig 2.** SEM image (a), diameter distribution (b), TEM image (c), and EDS analysis (d) of BiOI microspheres.

### 3.2. Optical properties

The optical properties of a semiconductor material are relevant to determine its photocatalytic activity. Therefore, the UV-vis diffuse reflectance spectra of BiOI sample were measured and then transformed to the corresponding absorption spectra through the Kubelka-Munk function (eq 1):

$$F(R_{\infty}) = \frac{1 - R_{\infty}}{2R_{\infty}} \quad (5)$$

Where  $R_{\infty} = \frac{R_{sample}}{R_{standard}}$  is the absolute reflectance of the sample and  $F(R_{\infty})$  is the remission function [25]. Afterward, the band gap energy was estimated by using the Tauc expression (eq 2):

$$(F(R_{\infty}) \cdot hv)^{1/\gamma} = B(hv - E_g) \quad (6)$$

where  $h$  the Plank constant,  $\nu$  the light vibration frequency,  $B$  a constant, and  $E_g$  the band gap energy. BiOI is a semiconductor characterized by its indirect allowed electron transition [24]. Owing to this property, the  $\gamma$  value used to calculate the band gap energy of BiOI microspheres was equal to 2. As can be observed in the Fig 3, the  $E_g$  value was estimated to be 2.22 eV. This implies that BiOI microspheres can absorb photons efficiently from the visible light corresponding to wavelengths equal to or less than 560 nm.

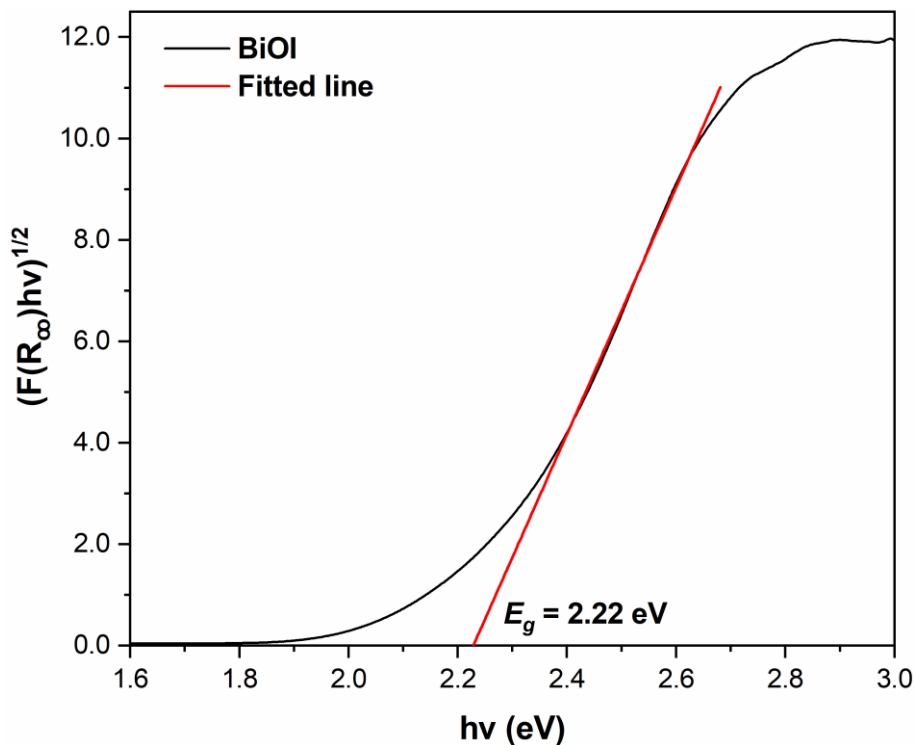


**Fig 3.** Plot of  $(F(R_{\infty}) \cdot hv)^{1/\gamma}$  versus the photon energy( $hv$ ).

### 3.3. Photoactivity of BiOI microspheres

The BPA test was the model target to verify that the BiOI microspheres are active in visible light and under the conditions in the photoreactor (i.e., room temperature, agitation). The BPA is a relatively recalcitrant endocrine disruptor that is commonly detected in water [26]. According to the Fig. S4, BiOI microspheres could degraded up to 90% of BPA, which indicates that they can be efficiently activated by the light from the LED lamp.

### **3.4. Photocatalytic reduction of nitrate**

#### **3.4.1. Effect of the photocatalyst dosage**

The photocatalytic activity depends on the amount of the photocatalyst. When the photocatalyst dosage is too high, the turbidity of the solution increases, blocking the absorption of light by the photocatalyst particles. In the same way, a photocatalyst dosage beyond an optimal concentration can lead to the agglomeration of the particles, resulting in low photocatalytic degradation. On the other hand, when the amount of photocatalyst particles is too low, the total active sites available on the surface of all particles are not enough to conduct the complete degradation of the pollutants[21]. Fig. 4a shows the photocatalytic reduction of 10 ppm of nitrate using different photocatalyst dosages and 0.004 M of formic acid as a hole scavenger. As expected, when no BiOI photocatalyst was added to the reaction medium (i.e., only formic acid), there was no nitrate reduction, which suggests that formic acid does not act as a reducing agent. Furthermore, there were no adsorption effects and no decrease in nitrate concentration was observed during the dark hour. However, it can be observed that by increasing the photocatalyst dosage, the reduction of nitrate also increases under light conditions. A reduction percentage of 18.5%, 30%, and 57% was obtained for 0.03, 0.06 and 0.13 g of photocatalyst, respectively, after 3 hours under white LED light irradiation. This effect is related with surface area available for the photocatalytic reactions and light absorption [27]. In other words, by increasing the photocatalyst dosage, the amount of active sites available for photon absorption increases, leading to a higher photogeneration of excited electrons for nitrate reduction[28]. Based on these results, 0.13 g of BiOI can be considered as the better photocatalyst dosage for reduction of nitrate under the experimental conditions given in this work. The experimental data obtained in the BiOI dosage test can be seen in Table 1S.

Additionally, the pH of the solution during the reduction of nitrate was measured over four hours of reaction. From Fig. 4b, it can be observed that as the nitrate concentration decreases, the pH of the solution increases. The acid environment in the beginning of the reaction has been related to the presence of formic acid. When using formic acid as a hole scavenger, it is common to have an initial pH of 2.5 to 3 [4], which is in accordance with the data obtained in this work (Table 2S).The increase of the pH during the reaction has been attributed to the consumption of  $H^+$  to form  $NO_2^-$  from  $NO_3^-$  [29].

For the case of 0.13 g BiOI, the pH rose quickly from 2.5 to 6.0 during the first 30 min of visible light irradiation, and slowly increased up to 7.2 in the last 150 min. This result had a positive correlation with the photocatalytic reduction of nitrate (Fig. 4a), in which the higher reduction rate occurred during the first 30 min of visible light irradiation. After then, the reduction rate declined, leading to less conversion of nitrate. This effect is due to the surface charge of the photocatalyst in the different pH values. The pH of point of zero charge (PZC) of BiOI microspheres is around of 2.9 [22], which means that in pH values higher than PZC the photocatalyst surface will have a negative charge. While in pH values smaller than PZC the photocatalyst surface will be charged positively. In this sense, the low photocatalytic reduction of nitrate by BiOI microspheres after 30 min of light illumination is due to the electrostatic repulsion between the nitrate anions and the negative charge of the photocatalyst surface.

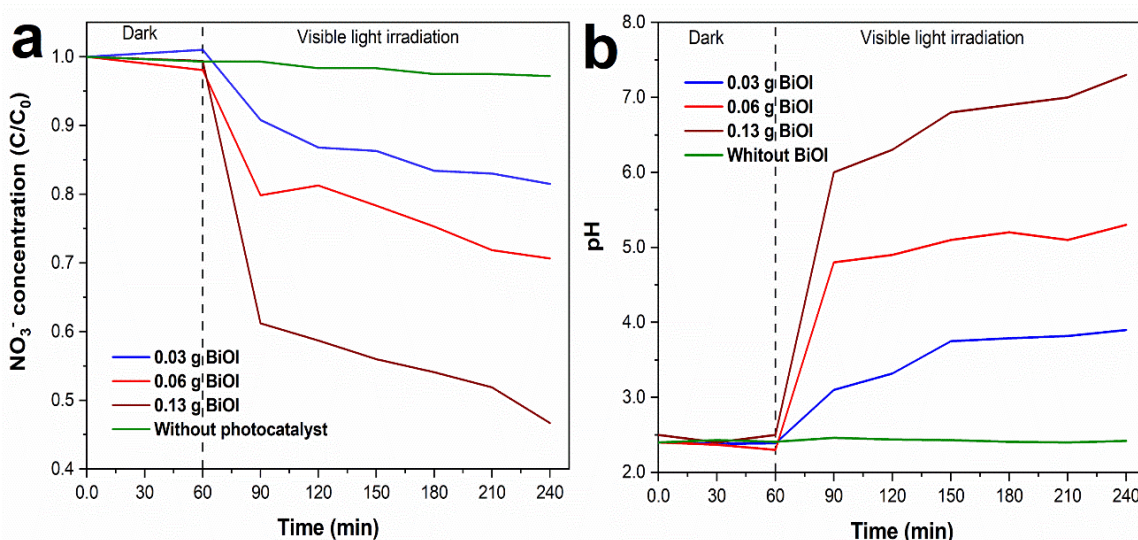
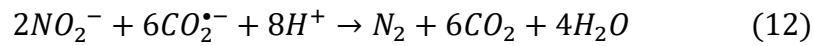
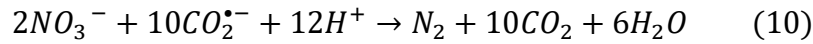
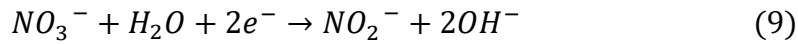
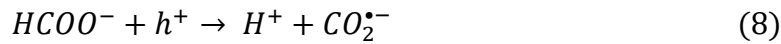


**Fig 4.** Effect of BiOI dosage on photocatalytic reduction of 10 ppm of nitrate under visible light irradiation (a), and changes of pH during the reaction (b).

### 3.4.2. Effect of addition of hole scavenger

The hole scavenger plays an important role during  $\text{NO}_3^-$  reduction, since it minimizes the recombination of the electron/hole pair and acts as a reduction process mediator [30]. Formic acid is one of the most studied hole scavenger for nitrate reduction due to its simple carboxylic acid structure and the direct one-electron transfer mechanism. Consequently, the formation of the strong reductant carboxylic anion radical ( $\text{CO}_2^{\bullet-}$ ) can be favored during

the reaction of formic acid with holes in the valence band of the photocatalyst. This helps in the degradation of nitrates by means of a reduction reaction. Moreover, formic acid is a weak acid with a pKa = 3.75, which implies that in pH values higher than 4.75 it can be deprotonated, releasing H<sup>+</sup>. Thus promoting the effective conversion of nitrate to molecular nitrogen [4]. Therefore, in presence of photocatalyst particles, nitrate molecules can be reduced by 3 pathways: (1) by direct interaction with electrons from the conduction band of the photocatalyst (eq 7-9), (2) by interaction with CO<sub>2</sub><sup>•-</sup> species (eq.10-11), and (3) by interaction with H<sup>+</sup> (eq. 10-11). In this sense, in the presence of formic acid, the photocatalytic reduction of nitrate to nitrogen could be expressed as follows (eq. 7-14) [8,28]



The CO<sub>2</sub><sup>•-</sup> radicals which are generated in the photocatalytic decomposition of formic acid (eq. 8) have strong reductive ability (E<sup>o</sup> (CO<sub>2</sub>/ CO<sub>2</sub><sup>•-</sup>) = 1.8V). CO<sub>2</sub><sup>•-</sup> species owing to their large reductive potential can efficiently reduce nitrate (E<sup>o</sup> (NO<sub>3</sub><sup>-</sup>/ NO<sub>2</sub><sup>-</sup>) =0.94V ; (E<sup>o</sup> (NO<sub>3</sub><sup>-</sup> / N<sub>2</sub>) =1.25 V); and E<sup>o</sup> (NO<sub>2</sub><sup>-</sup>/ N<sub>2</sub>) =1.45V ) to nitrogen [10].

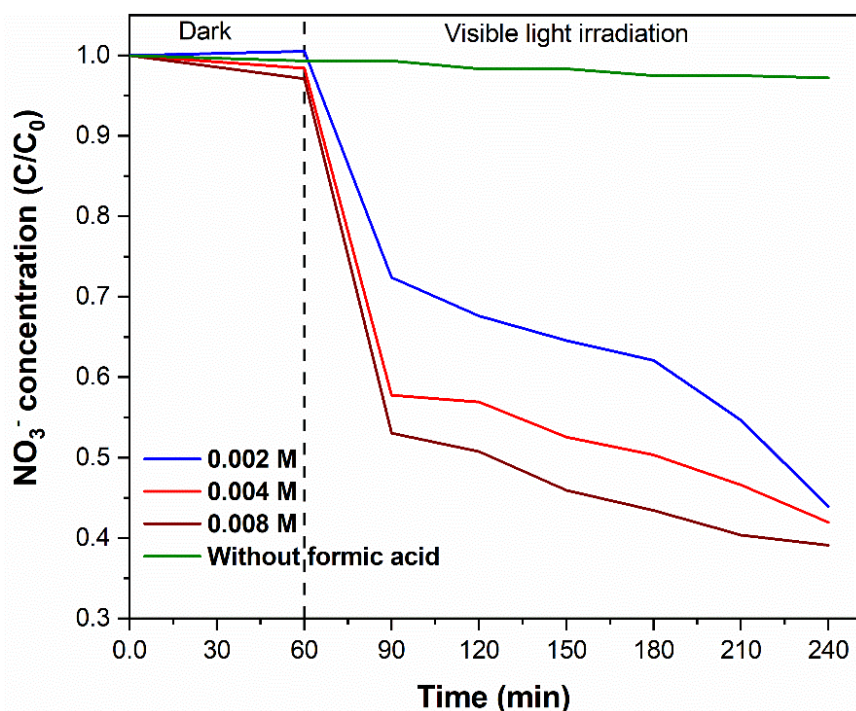


**Fig 5.** Effect of formic acid concentration as a hole scavenger on photocatalytic reduction of 10 ppm of nitrate using 0.13 g of BiOI under visible light illumination.

The optimal concentration of formic acid as a hole scavenger depends on the catalytic sites available on the photocatalyst surface, and the nitrate source [31]. In this work, 3 different concentrations of formic acid were analyzed using 0.13 g of BiOI. Fig 5. shows that a better reduction of nitrate is obtained with 0.008M of acid formic under the given reaction conditions; probably due to the higher formation of  $\text{CO}_2^{\bullet-}$  radicals and higher number of electrons available. Also, when the experiment was performed without formic acid, no reduction reaction occurred. This suggests that the photocatalyst cannot carry out reduction processes on its own, it needs a hole scavenger. Moreover, it can be seen that with 0.002 M of formic acid the reduction of nitrate was affected. In this regard, it has been reported that low concentrations of formic acid can lead to an incomplete nitrate reduction and insufficient reducing mediators  $\text{CO}_2^{\bullet-}$  [28], which in turn can result in a higher recombination rate of photogenerated electrons and holes, and thereby, low nitrate reduction [32]. Therefore, these results reveal that 0.008 M is the best concentration of formic acid for nitrate reduction compared with 0.004 and 0.002 M.

### 3.5. Selectivity of the photocatalytic reduction of $\text{NO}_3^-$

The photocatalytic removal efficiency ( $e$ ) of nitrate,  $\text{N}_2$  selectivity ( $s_{\text{N}_2}$ ),  $\text{NH}_4^+$  selectivity ( $s_{\text{NH}_4^+}$ ), and  $\text{NO}_2^-$  selectivity ( $s_{\text{NO}_2^-}$ ) using 0.13 g of BiOI photocatalyst with different

formic acid concentrations were determined by using the equations 1-4 described in the section 2.5 and using the experimental data of Table 3S. According to the  $e$  values listed in Table 1, the nitrate removal efficiency improved with the increase in formic acid concentration. This result had a positive correlation with the increase in nitrogen selectivity.

**Table 1.** Removal efficiency and selectivity of photocatalytic reduction using BiOI microspheres.

Formic acid [M]	$e$ (%)	$s\text{NO}_2^-$ (%)	$\text{NH}_4^+$ (%)	$s\text{N}_2$ (%)
<b>0.008</b>	60.87	0	0.1757	99.82
<b>0.004</b>	58.60	0	3.8409	96.16
<b>0.002</b>	56.05	10.04	7.3864	82.58

The selectivity towards nitrogen ( $s\text{N}_2$ ) is defined as the ratio between the concentration of nitrate reduced to form nitrogen and the total concentration of nitrate reduced, considering that no by-products other than nitrite ( $\text{NO}_2^-$ ) and ammonium ( $\text{NH}_4^+$ ) are formed [32]. The following numbers were calculated from the data of the measurements of ion chromatography (Table 3S). It can be seen that better results are obtained using 0.008 M formic acid. Using this hole scavenger concentration, the  $\text{N}_2$  selectivity was 99.82 %, which is in accordance with the higher  $s\text{NO}_2^-$  and  $s\text{NH}_4^+$ , and absence of  $\text{NO}_2^-$  and  $\text{NH}_4^+$  ions at the end of the reaction (Fig. 6). A confirmation that the final product is  $\text{N}_2$  and not  $\text{N}_2\text{O}$  or  $\text{NO}$ , would require gas analysis, and therefore, for a substantial change in the experimental design. This is beyond the scope of the presented research, which aims to identify possible candidates for the photocatalytic reduction of nitrate under visible light.

In a recent study, a nitrate reduction percentage of 40% and  $\text{N}_2$  selectivity of 13.2% were obtained by using BiOCl nanosheets as photocatalyst, and a 500 W Xenon lamp as visible light source [19]. To further increase nitrate removal, they prepared a series of BiOCl<sub>n</sub>Br<sub>1-n</sub> ( $0 \leq n \leq 1$ ) nanosheets with different Cl/Br ratios, and they achieve a nitrate conversion to  $\text{N}_2$  of about 90% after 5 h of visible light irradiation. The reduction rate obtained with BiOCl<sub>n</sub>Br<sub>1-n</sub> nanosheets is higher than that obtained with the synthesized BiOI microspheres. In our experiment, the nitrate conversion was only 57%. This may be due to

the lower light intensity of the 50 W LED lamp used in this work, compared to the 500 W Xenon lamp in the mentioned study. However, we want to point out that the LED lamps not only consumes less energy, it is also easier to handle and more energy-efficient because of lower heat production compared with a 500 W Xenon lamp. This is important for practical applications at laboratory scale as well as at large-scale to decrease the water treatment costs.

To achieve optimal photocatalytic nitrate conversion, it is important to completely remove the dissolved oxygen from the reaction medium. It is well known that dissolved oxygen has a high electron affinity, which means that in photocatalytic processes can act as a scavenger of the photoexcited electrons. In order to ensure a complete reduction and conversion of nitrate to nitrogen is required a high amount of available photoexcited electrons. When the dissolved oxygen (DO) is present in the reaction, the oxygen molecules compete with nitrate for the available electrons, thus decreasing the reduction percentage and N<sub>2</sub> selectivity. In this study, an initial concentration of 4.5 mg/L of DO was obtained and the sonication method was able to reduce this concentration to approximately 1.7 mg/L, more than 50% (Fig S5). However, since the dissolved oxygen could not be completely eliminated, these could interfere with the reaction and, therefore, a higher percentage of reduction could not be achieved. Argon and nitrogen gas has been used in some studies to remove completely the dissolved oxygen and, thereby, to increase the reduction rate of nitrate [27–29]. However, we can see that despite not completely eliminating dissolved oxygen from the solution, we were able to achieve a fairly high nitrate reduction compared to other studies [19].

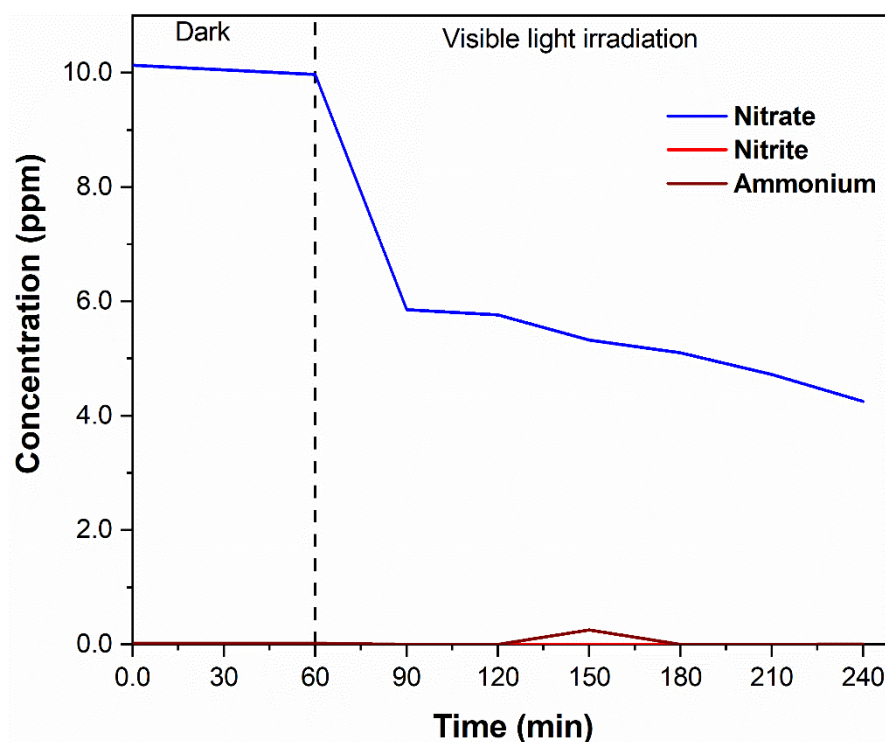


**Fig 6.** Concentration curve of  $NO_3^-$ , formed  $NO_2^-$  and  $NH_4^+$  plotted as a function of irradiation time with 0.008 M of formic acid and 0.13 g of BiOI.

#### 4. Conclusions

BiOI flower-like microspheres, obtained by a solvothermal method, were found to be effective in the photocatalytic reduction of nitrate in a slurry reactor under visible LED light irradiation. The products were analyzed by ion chromatography and low concentrations of nitrite and ammonium were detected. The reaction depends on the amount of added photocatalyst (more = better), the pH of the solution, the concentration of dissolved oxygen, and the hole scavenger concentration. 0.008 M of acid formic showed better results than lower concentrations. This work indicates that BiOI flower-like microspheres can be potential photocatalysts for nitrate reduction, and this may be the baseline for further investigations using this type of photocatalyst for reduction processes.

#### Acknowledgments

Thanks to Inedita (Senescyt, Ecuador) PIC-18-INE-IKIAM-001, Laboratorio de Referencia Nacional del Agua, and Ikiam University technicians and facility manager.

## References

- [1] M.H. Ward, T.M. deKok, P. Levallois, J. Brender, G. Gulis, B.T. Nolan, J. VanDerslice, Workgroup report: Drinking-water nitrate and health - Recent findings and research needs, *Environ. Health Perspect.* 113 (2005) 1607–1614. <https://doi.org/10.1289/ehp.8043>.
- [2] V. Matějů, S. Čížinská, J. Krejčí, T. Janoch, Biological water denitrification-A review, *Enzyme Microb. Technol.* 14 (1992) 170–183. [https://doi.org/10.1016/0141-0229\(92\)90062-S](https://doi.org/10.1016/0141-0229(92)90062-S).
- [3] L. Fewtrell, Drinking-water nitrate, methemoglobinemia, and global burden of disease: A discussion, *Environ. Health Perspect.* 112 (2004) 1371–1374. <https://doi.org/10.1289/ehp.7216>.
- [4] H.O.N. Tugaoen, S. Garcia-Segura, K. Hristovski, P. Westerhoff, Challenges in photocatalytic reduction of nitrate as a water treatment technology, *Sci. Total Environ.* 599–600 (2017) 1524–1551. <https://doi.org/10.1016/j.scitotenv.2017.04.238>.
- [5] D. Contreras, V. Melin, G. Pérez-González, A. Henríquez, L. González, Advances and Challenges in BiOX (X: Cl, Br, I)-Based Materials for Harvesting Sunlight, en: 2020: pp. 235–282. [https://doi.org/10.1007/978-3-030-15608-4\\_10](https://doi.org/10.1007/978-3-030-15608-4_10).
- [6] A. Sowmya, S. Meenakshi, Photocatalytic reduction of nitrate over Ag-TiO<sub>2</sub> in the presence of oxalic acid, *J. Water Process Eng.* 8 (2015) e23–e30. <https://doi.org/10.1016/j.jwpe.2014.11.004>.
- [7] F. Zhang, R. Jin, J. Chen, C. Shao, W. Gao, L. Li, N. Guan, High photocatalytic activity and selectivity for nitrogen in nitrate reduction on Ag/TiO<sub>2</sub> catalyst with fine silver clusters, *J. Catal.* 232 (2005) 424–431. <https://doi.org/10.1016/j.jcat.2005.04.014>.
- [8] Y.A. Shaban, A.A. El Maradny, R.K. Al Farawati, Photocatalytic reduction of nitrate in seawater using C/TiO<sub>2</sub> nanoparticles, *J. Photochem. Photobiol. A Chem.* 328 (2016) 114–121. <https://doi.org/10.1016/j.jphotochem.2016.05.018>.
- [9] J.B. Islam, M. Furukawa, I. Tateishi, S. Kawakami, H. Katsumata, S. Kaneco, Enhanced photocatalytic reduction of toxic Cr(VI) with Cu modified ZnO nanoparticles in presence of EDTA under UV illumination, *SN Appl. Sci.* 1 (2019) 1–11. <https://doi.org/10.1007/s42452-019-1282-x>.
- [10] J. Sá, C.A. Agüera, S. Gross, J.A. Anderson, Photocatalytic nitrate reduction over metal modified TiO<sub>2</sub>, *Appl. Catal. B Environ.* 85 (2009) 192–200. <https://doi.org/10.1016/j.apcatb.2008.07.014>.
- [11] N. Krasae, K. Wantala, Enhanced nitrogen selectivity for nitrate reduction on Cu–nZVI by TiO<sub>2</sub> photocatalysts under UV irradiation, *Appl. Surf. Sci.* 380 (2016) 309–317. <https://doi.org/10.1016/J.APSUSC.2015.12.023>.
- [12] J.M.A. Freire, M.A.F. Matos, D.S. Abreu, H. Becker, I.C.N. Diógenes, A. Valentini, E. Longhinotti, Nitrate photocatalytic reduction on TiO<sub>2</sub>: Metal loaded, synthesis and anions effect, *J. Environ. Chem. Eng.* 8 (2020) 103844. <https://doi.org/10.1016/J.JECE.2020.103844>.

- [13] S.U.M. Khan, M. Al-Shahry, W.B. Ingler, Efficient photochemical water splitting by a chemically modified n-TiO<sub>2</sub>, *Science* (80-. ). (2002). <https://doi.org/10.1126/science.1075035>.
- [14] R. Meribout, Y. Zuo, A.A. Khodja, A. Piram, S. Lebarillier, J. Cheng, C. Wang, P. Wong-Wah-Chung, Photocatalytic degradation of antiepileptic drug carbamazepine with bismuth oxychlorides (BiOCl and BiOCl/AgCl composite) in water: Efficiency evaluation and elucidation degradation pathways, *J. Photochem. Photobiol. A Chem.* 328 (2016) 105–113. <https://doi.org/10.1016/j.jphotochem.2016.04.024>.
- [15] X. Gao, W. Peng, G. Tang, Q. Guo, Y. Luo, Highly efficient and visible-light-driven BiOCl for photocatalytic degradation of carbamazepine, *J. Alloys Compd.* 757 (2018) 455–465. <https://doi.org/10.1016/j.jallcom.2018.05.081>.
- [16] Y.I. Choi, Y. Il Kim, D.W. Cho, J.S. Kang, K.T. Leung, Y. Sohn, Recyclable magnetic CoFe<sub>2</sub>O<sub>4</sub>/BiOX (X = Cl, Br and I) microflowers for photocatalytic treatment of water contaminated with methyl orange, rhodamine B, methylene blue, and a mixed dye, *RSC Adv.* 5 (2015) 79624–79634. <https://doi.org/10.1039/c5ra17616f>.
- [17] D. Wu, S. Yue, W. Wang, T. An, G. Li, H.Y. Yip, H. Zhao, P.K. Wong, Boron doped BiOBr nanosheets with enhanced photocatalytic inactivation of *Escherichia coli*, *Appl. Catal. B Environ.* 192 (2016) 35–45. <https://doi.org/10.1016/j.apcatb.2016.03.046>.
- [18] Y. Li, J. Wang, H. Yao, L. Dang, Z. Li, Efficient decomposition of organic compounds and reaction mechanism with BiOI photocatalyst under visible light irradiation, *J. Mol. Catal. A Chem.* 334 (2011) 116–122. <https://doi.org/10.1016/J.MOLCATA.2010.11.005>.
- [19] J. Di, J. Xia, Y. Ge, L. Xu, H. Xu, M. He, Q. Zhang, H. Li, Reactable ionic liquid-assisted rapid synthesis of BiOI hollow microspheres at room temperature with enhanced photocatalytic activity, *J. Mater. Chem. A.* 2 (2014) 15864–15874. <https://doi.org/10.1039/c4ta02400a>.
- [20] X.J. Wang, Y.Q. Song, J.Y. Hou, X.N. Chen, Fabrication of BiOI Hierarchical Microspheres with Efficient Photocatalysis for Methylene Blue and Phenol Removal, *Cryst. Res. Technol.* 52 (2017) 1–7. <https://doi.org/10.1002/crat.201700068>.
- [21] L. Wang, S. qi Guo, Y. Chen, M. Pan, E.H. Ang, Z. hao Yuan, A Mechanism Investigation of how the Alloying Effect Improves the Photocatalytic Nitrate Reduction Activity of Bismuth Oxyhalide Nanosheets, *ChemPhotoChem.* 4 (2020) 110–119. <https://doi.org/10.1002/cptc.201900217>.
- [22] A.C. Mera, C.A. Rodríguez, M.F. Meléndrez, H. Valdés, Synthesis and characterization of BiOI microspheres under standardized conditions, *J. Mater. Sci.* 52 (2017) 944–954. <https://doi.org/10.1007/s10853-016-0390-x>.
- [23] J. Schullehner, L. Stayner, B. Hansen, Nitrate, nitrite, and ammonium variability in drinking water distribution systems, *Int. J. Environ. Res. Public Health.* 14 (2017) 1–9. <https://doi.org/10.3390/ijerph14030276>.

- [24] A.C. Mera, Y. Moreno, J.Y. Pivan, O. Peña, H.D. Mansilla, Solvothermal synthesis of BiOI microspheres: Effect of the reaction time on the morphology and photocatalytic activity, *J. Photochem. Photobiol. A Chem.* 289 (2014) 7–13. <https://doi.org/10.1016/J.JPHOTOCHEM.2014.05.015>.
- [25] V. Džimbeg-Malčić, Ž. Barbarić-Mikočević, K. Itrić, Kubelka-Munk theory in describing optical properties of paper (II), *Teh. Vjesn.* 19 (2012) 191–196.
- [26] J. Im, F.E. Löffler, Fate of Bisphenol A in Terrestrial and Aquatic Environments, *Environ. Sci. Technol.* 50 (2016) 8403–8416. <https://doi.org/10.1021/acs.est.6b00877>.
- [27] O. Rojviroon, S. Sirivithayapakorn, T. Rojviroon, C. Wantawin, Effects of Initial Nitrate Concentrations and Photocatalyst Dosages on Ammonium Ion in Synthetic Wastewater Treated by Photocatalytic Reduction, (2020). <https://doi.org/10.1155/2020/8893816>.
- [28] Z. Geng, Z. Chen, Z. Li, X. Qi, X. Yang, W. Fan, Y. Guo, L. Zhang, M. Huo, Enhanced photocatalytic conversion and selectivity of nitrate reduction to nitrogen over AgCl/TiO<sub>2</sub> nanotubes, *Dalt. Trans.* 47 (2018) 11104–11112. <https://doi.org/10.1039/c8dt01915k>.
- [29] Y. Liu, X. Gong, W. Yang, B. Wang, Z. Yang, Y. Liu, Selective Reduction of Nitrate into Nitrogen Using Cu/Fe Bimetal Combined with Sodium Sulfite, *Ind. Eng. Chem. Res.* 58 (2019) 5175–5185. <https://doi.org/10.1021/acs.iecr.8b05721>.
- [30] K. Doudrick, T. Yang, K. Hristovski, P. Westerhoff, Photocatalytic nitrate reduction in water: Managing the hole scavenger and reaction by-product selectivity, *Appl. Catal. B Environ.* 136–137 (2013) 40–47. <https://doi.org/10.1016/j.apcatb.2013.01.042>.
- [31] K. Doudrick, T. Yang, K. Hristovski, P. Westerhoff, Photocatalytic nitrate reduction in water: Managing the hole scavenger and reaction by-product selectivity, *Appl. Catal. B Environ.* 136–137 (2013) 40–47. <https://doi.org/10.1016/j.apcatb.2013.01.042>.
- [32] D. de Bem Luiz, H.J. José, R. de F. Peralta Muniz Moreira, Kinetics of photocatalytic reduction of nitrate in synthetic and real effluent using TiO<sub>2</sub> doped with Zn as photocatalyst, *J. Chem. Technol. Biotechnol.* 90 (2015) 821–829. <https://doi.org/10.1002/jctb.4375>.
- [33] O.S.G.P. Soares, M.F.R. Pereira, J.J.M. Órfão, J.L. Faria, C.G. Silva, Photocatalytic nitrate reduction over Pd-Cu/TiO<sub>2</sub>, *Chem. Eng. J.* 251 (2014) 123–130. <https://doi.org/10.1016/j.cej.2014.04.030>.

Supplementary Information

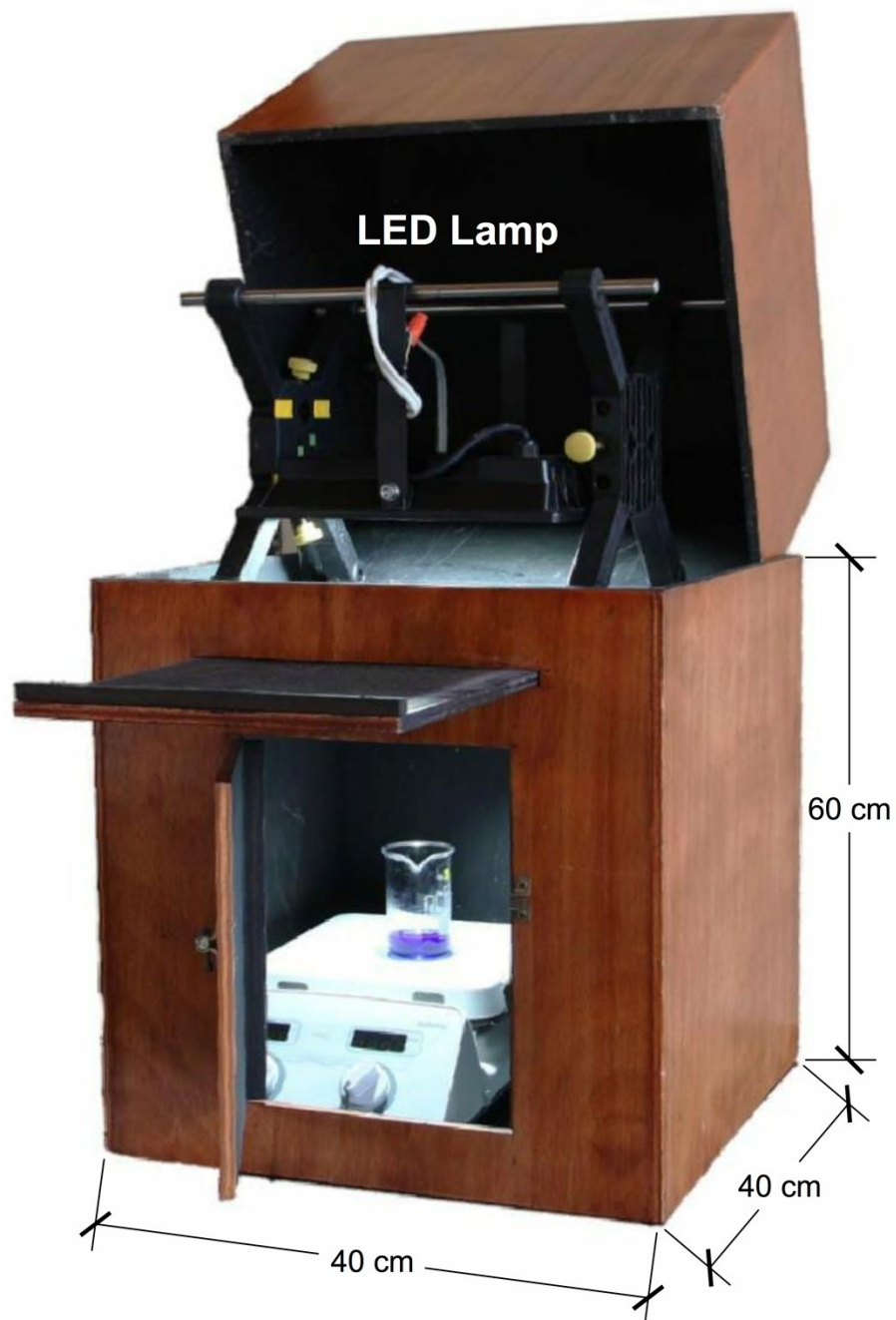


**Fig S1.** Photoreactor dimensions with opened front and "ON/OFF" door.

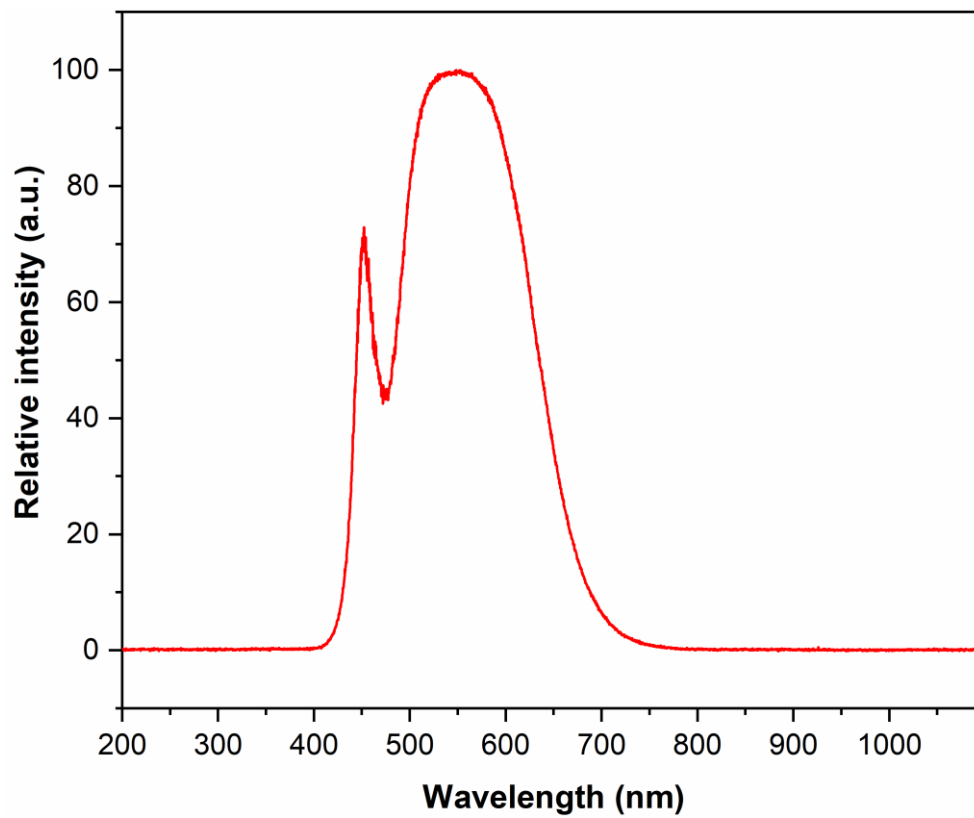


**Fig S2.** Spectra of the 50 W white LED lamp.

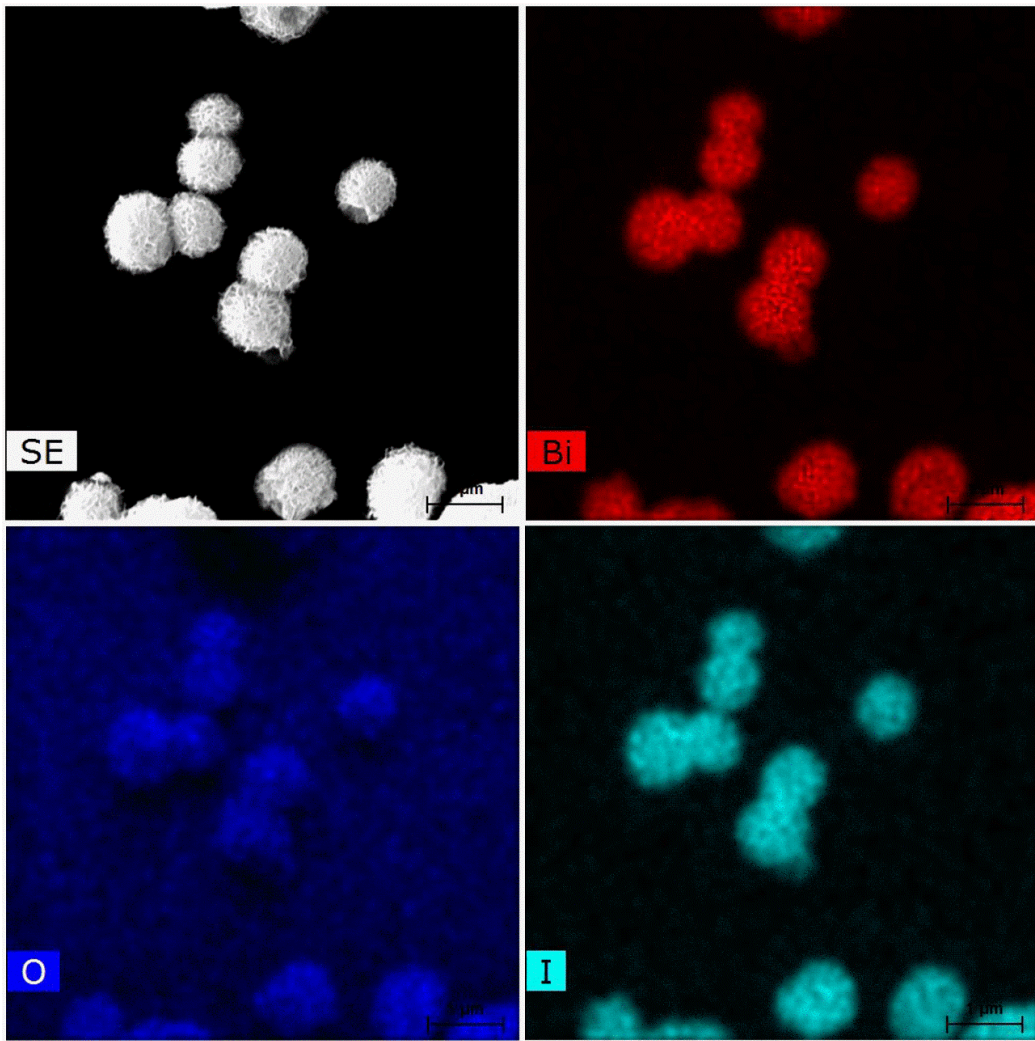


**Fig S3.** EDS mapping of BiOI sample

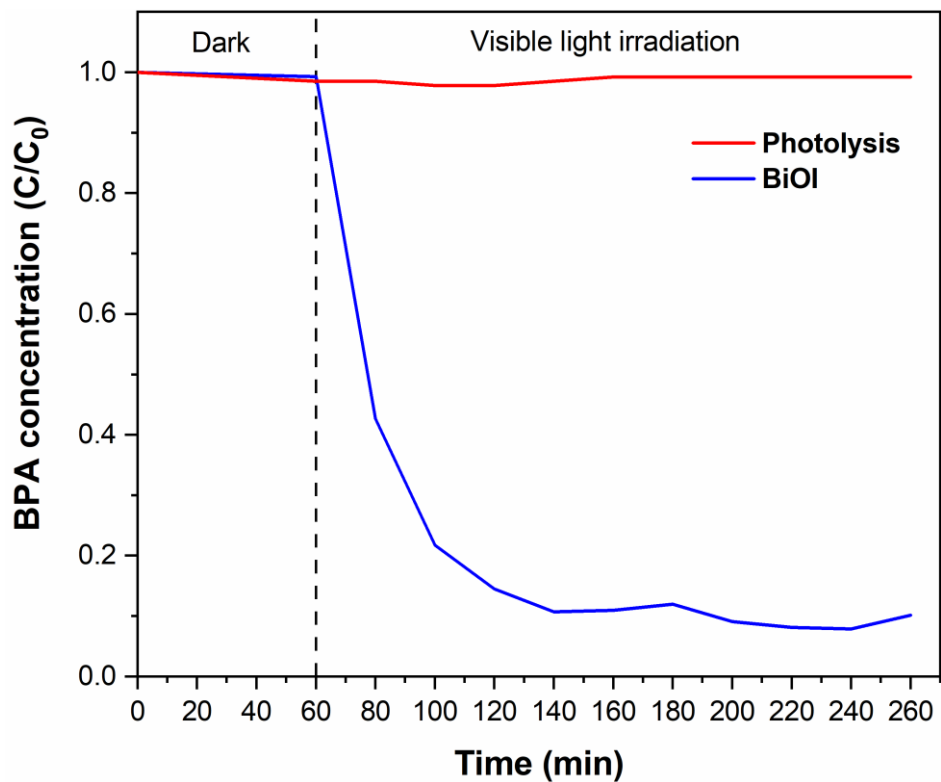


Fig S4. Photocatalytic degradation of BPA by BiOI microspheres under white LED light irradiation.

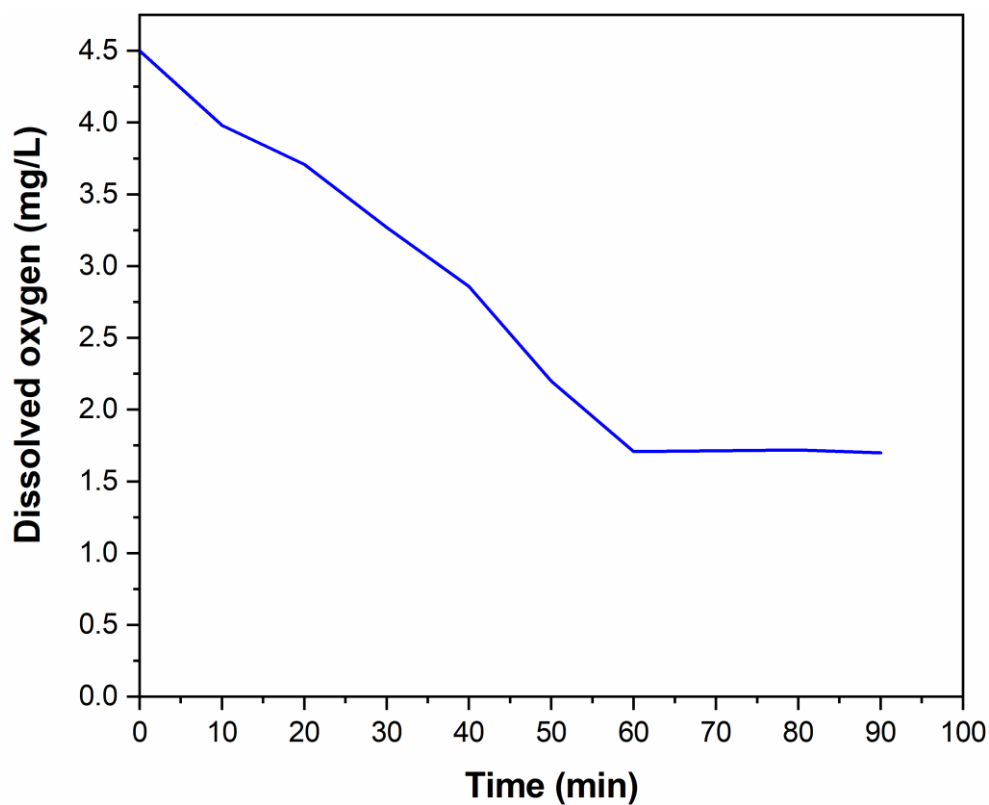


Fig S5. Dissolved oxygen removal through sonication. Concentration values were measured using a multiparameter (YSI).

**Table 1S.** Experimental data on the effect of the photocatalyst dosage

		Reaction time (min)							
Assay	Ion	0	60	90	120	150	180	210	240
Dark	Nitrate	1	0.98	0	0.97	0	0.97	0	0.98
	Ammonium	0	0		0		0		0
	Nitrite	1	1	0	1	0	1	0	1
Photolysis	Nitrate	1	0.99	0	0.98	0	0.97	0	0.97
	Ammonium	0	0		0		0		0
	Nitrite	0	0		0		0		0
		Dark			Visible Light				
30 mg BiOI	Nitrate	1	1.01	0.91	0.87	0.86	0.83	0.83	0.81
	Ammonium	0	0	0	0	0	0	0	0
	Nitrite	0	0	0	0	0	0	0	0
60 mg BiOI	Nitrate	1	0.98	0.79	0.81	0.78	0.75	0.71	0.71
	Ammonium	1	0	0	1.03	2.28	1.73	0	0
	Nitrite	0	0	0	0	0	0	0	0
130 mg BiOI R1	Nitrate	1	0.99	0.61	0.58	0.56	0.54	0.51	0.47
	Ammonium	0	0	0	0	1	0	0	0.04
	Nitrite	0	0	1	0	0	0	0	0
130 mg BiOI R2	Nitrate	1	0.96	0.52	0.55	0.48	0.46	0.41	0.38
	Ammonium	1	0.08	0	0	0.36	0	0	0
	Nitrite	0	0	0	0	0	0	0	0
130 mg BiOI R3	Nitrate	1	0.99	0.60	0.57	0.53	0.51	0.46	0.41
	Ammonium	0	0	0	0	1	0	0	0.043
	Nitrite	0	0	0	0	0	0	0	0

**Table 2S.** Experimental data of pH during the reaction of nitrate reduction

Hole Scavenger	Assay	Reaction time (min)								
		0	30	60	90	120	150	180	210	240
Formica cid 0.004 M	30 mg BiOI	2.4	2.38	2.39	3.1	3.32	3.75	3.79	3.82	3.9
	60 mg BiOI	2.4	2.37	2.3	4.8	4.9	5.1	5.2	5.1	5.3
	130 mg BiOI	2.5	2.4	2.5	6	6.3	6.8	6.9	7	7.3

**Table 3S.** Experimental data of effect of different concentrations of formic acid

Reaction time (min)									
Formic acid	Ion	0	60	90	120	150	180	210	240
0.008 M	Nitrate	1	0.9712	0.5304	0.5077	0.4593	0.4346	0.4037	0.3913
	Ammonium	0	1	2.5333	0	0	0	0	15.1333
	Nitrite	0	0	1	1.1795	0	0	0	0
0.002 M	Nitrate	1	1.0053	0.7240	0.6762	0.6454	0.6210	0.5467	0.4395
	Ammonium	1	1.3175	0	0	0	1.2540	3.4127	6.1905
	Nitrite	0	1	0.7206	0.6765	1.0147	0.7206	0.3529	0.7794
0.004 M	Nitrate	1	0.9654	0.5248	0.5510	0.4846	0.4621	0.4191	0.3807
	Ammonium	1	0.0844	0	0	0.3689	0	0	0
	Nitrite	0	0	0	0	0	0	0	0
Without	Nitrate	1	0.9932	0	0.9836	0	0.9749	0	0.9720
	Ammonium	0	0	0	0	0	0	0	0
	Nitrite	0	0	0	0	0	0	0	0